(1979) *Anal. Biochem. 99*, 72–84.
Moore, D. G., & Koshland, D. E. (1967) *J. Biol. Chem. 262*, 2447–2452.
Nakamura, Y., Nakajima, S., & Grundfest, H. (1965) *J. Gen. Physiol. 49*, 321–349.
Narahashi, T., Anderson, N. C., & Moore, J. S. (1967) *J. Gen. Physiol. 50*, 1413–1428.
Radin, M. A. (1969) *Methods Enzymol. 14*, 482–530.
Reed, J., & Raftery, M. A. (1976) *Biochemistry 15*, 944–953.
Ritchie, J. M., & Rogart, R. B. (1977) *Rev. Physiol., Biochem. Pharmacol. 79*, 1–50.
Ritchie, J. M., Rogart, R. B., & Strichartz, G. (1976) *J. Physiol. 261*, 477–494.
Sigworth, F. J. (1980) *J. Physiol. 307*, 131–142.
Sigworth, F. J., & Spaulding, B. C. (1979) *Nature (London) 283*, 293.
Udenfriend, S., Stein, S., Bahleu, P., Dairman, W., Leimgruber, W., & Weigele, M. (1972) *Science (Washington, D.C.) 178*, 871–873.
Ulbricht, W. (1977) *Annu. Rev. Biophys. Bioeng. 6*, 7–31.
Ulbricht, W., & Wagner, H.-H. (1975) *Philos. Trans. R. Soc. London, Ser. B 270*, 353–364.

Molecular Dynamics and Conformation in the Gel and Liquid-Crystalline Phases of Phosphatidylethanolamine Bilayers†

A. Blume,‡ D. M. Rice, R. J. Wittebort,§ and R. G. Griffin*

ABSTRACT: Solid-state deuterium and carbon-13 nuclear magnetic resonance (NMR) spectra have been used to study the molecular dynamics and conformation of dipalmitoylphosphatidylethanolamine (DPPE) in both the gel (L_β) and liquid-crystalline (L_α) phases. For this purpose DPPE was labeled with ^{13}C in the carbonyl group of the *sn*-2 chain and with ^2H at three different positions—4, 8, and 12—of the *sn*-2 chain, at the 2 position of the glycerol backbone, and at the 1 position of the ethanolamine head group. The ^{13}C carbonyl and ^2H chain spectra indicate that in the gel phase the DPPE molecules are diffusing about their long axes at rates of 10^5–10^6 s^{-1} and the acyl chains are in an approximately all-trans conformation. The glycerol backbone spectra suggest that the backbone is in a gauche conformation in the gel state, rather than a trans conformation such as found in single crystals. The head group spectra in the gel phase are broad, featureless lines of about 20-kHz width. At the $L_\beta \rightarrow L_\alpha$ phase transition several changes take place. As is well-known, the chains disorder, and fast long-axis rotational diffusion begins, which results in the sharp, axially symmetric L_α phase ^2H spectra, which are a factor of 2 narrower than those observed in the L_β phase. The head group spectra also sharpen substantially at the transition, although their total width remains approximately constant. The invariance of the spectral width suggests that the average head group conformation is similar in both phases. However, the sharper spectra seen in the L_α phase indicate that the rates of the head group motions in this phase are at least 3 orders of magnitude faster than those in the L_β phase. Thirdly, the ^2H spectra of the glycerol backbone labeled DPPE narrow by a factor of about 4, and we believe this is due to a conformational change in this region of the molecule. Consistent with this interpretation is the fact that the powder pattern exhibited by the *sn*-2 $^{13}C{=}O$ in the L_β phase collapses to an isotropic-like line at the phase transition.

Deuterium nuclear magnetic resonance (^2H NMR)[1] has been used extensively to examine the structural and dynamical properties of phospholipid bilayers in the L_α or liquid-crystalline phase. For example, the acyl chains in PC's and PS, the glycerol backbone in PC's and PE's, and the head groups of four different lipid classes have been studies with this technique (Seelig & Seelig, 1974, 1975; Seelig, 1977; Oldfield et al., 1978; Browning & Seelig, 1980). The results of these investigations suggest that phospholipids in the liquid-crystalline phase generally exhibit similar behavior. For instance, the acyl chain spectra show a plateau region with quadrupole splittings of about 30 kHz, which decrease as the terminal methyl group is approached. Spectra of head group labeled lipids differ in detail as might be expected; however, in all cases they are relatively narrow, axially symmetric powder line shapes, which suggests greater conformational freedom than is available in the acyl chain region of the bilayer (Seelig & Seelig, 1980).

In contrast to the liquid-crystalline phase, the gel phase of phospholipids has been much less thoroughly examined. The reason for this is partially due to the technical difficulties associated with obtaining gel-state ^2H NMR spectra, which are a factor of 2–4 times wider than those observed in the liquid-crystalline phase. However, with the introduction of the quadrupole echo technique (Solomon, 1958; Davis et al.,

† From the Francis Bitter National Magnet Laboratory, Massachusetts Institute of Technology, Cambridge, Massachusetts 02139. *Received February 25, 1982; revised manuscript received July 8, 1982.* This research was supported by the National Institutes of Health (GM-23289, GM-25505, and RR-00995) and by the National Science Foundation through its support of the Francis Bitter National Magnet Laboratory (C-670). A.B. was supported by a research scholarship from the Deutsche Forschungsgemeinschaft (BL 182/2-4) and R.J.W. by a U.S. Public Health Service postdoctoral fellowship (GM-07215).

‡ Present address: Institut für physikalische Chemie II, D-7800 Freiburg, Federal Republic of Germany.

§ Present address: Department of Chemistry, University of Louisville, Louisville, KY 60292.

[1] Abbreviations: DPPE, dipalmitoylphosphatidylethanolamine; DPPC, dipalmitoylphosphatidylcholine; DLPE, dilauroylphosphatidylethanolamine; DMPC, dimyristoylphosphatidylcholine; PC, phosphatidylcholine; PS, phosphatidylserine; PE, phosphatidylethanolamine; ^2H NMR, deuterium nuclear magnetic resonance; TLC, thin-layer chromatography; ESR, electron spin resonance.

0006-2960/82/0421-6220$01.25/0

1976) reports of gel-state spectra have begun to appear. Davis (1979) examined DPPC with perdeuterated acyl chains and concluded that the chains of this lecithin were probably in an all-trans conformation and executing axial diffusion about the molecular long axis. However, because of spectral overlap, a detailed analysis of the line shapes was not possible. Very different results were recently described by Huang et al. (1980) for specifically labeled glycolipid bilayers. In this case the spectral line shapes were total axially asymmetric—the asymmetry parameter, η, was unity—and these were interpreted in terms of a motional model involving restricted trans–gauche isomerization.

In this paper we report ^2H and ^{13}C NMR studies of bilayers of DPPE designed to elucidate the conformation and dynamics of PE molecules in both the gel and liquid-crystalline phases. This lipid was chosen for these investigations for several reasons. First, PE's are one of the major classes of lipids found in biological membranes. For example, the red blood cell membrane and virial membranes (Rothman & Lenard, 1977) and the cell membranes of *Escherichia coli* (Overath & Thilo, 1978) are all known to contain substantial amounts of PE. Second, the phase behavior of PE's with saturated acyl chains is, in comparison with that of PC's, relatively simple. It is well-known that diacyl-PC's exhibit a pretransition (Chapman et al., 1967), in addition to the main thermotropic phase transition. With ^{13}C spectroscopy it has recently been demonstrated (Wittebort et al., 1981, 1982) that this pretransition, and the formation of the monoclinic phase (Janiak et al., 1976, 1979), results in at least two different conformations of lipid molecules in the bilayer. Thus, an interpretation of the ^2H acyl chain spectra must account for these two types of conformationally inequivalent molecules, and their internal degrees of freedom, which are most likely not identical. Furthermore, a third "subtransition" has recently been reported for DPPC after incubation of the dispersions at 0 °C (Chen et al., 1980). In contrast, the phase behavior in DPPE is much less complicated in that at pH 7 a single transition from the gel to the liquid-crystalline phase is observed. We will see below that this results in ^{13}C and ^2H spectra that can be satisfactorily simulated by assuming a single population of lipid molecules in the bilayer. Finally, PE's exhibit a higher transition temperature than the corresponding PC's (Chapman et al., 1974; Blume & Ackermann, 1974; Vaughan & Keough, 1974, Mabrey & Sturtevant, 1976; Blume, 1979); thus, a large temperature range below the gel–liquid-crystalline phase transition can be studied without the necessity of cooling below the freezing point of water. Because of these properties, DPPE bilayers are an attractive model system for investigations of the conformational and motional behavior of glycerol phospholipids in the gel phase, and the manner in which they transform to the liquid-crystalline state.

Accordingly, we have prepared three ^2H chain labeled DPPE's—namely, the 4,4-, 8,8-, and 12,12-$^2H_2$ compounds—where the ^2H label is on the *sn*-2 chain. The spectra of these molecules suggest that in the L_β phase DPPE chains are in an approximately all-trans conformation. Moreover, simulations of the spectral lines shapes indicate that they are diffusing about their molecular long axis at rates of 10^5–10^6 s^{-1}. In addition, we have found in studies of other glycerol phospholipids that the glycerol backbone may undergo a conformational change at the gel–liquid-crystalline phase transition (Wittebort et al., 1981, 1982). Thus, we have examined spectra of DPPE ^{13}C labeled at the *sn*-2 carbonyl and at the 2 position of the glycerol backbone. The results suggest that the glycerol backbone in the gel state is in a gauche conformation, while in the liquid-crystalline phase a different conformation is preferred. Finally, we have studied DPPE ^2H labeled in the head group. The head group spectra in the gel phase are severely broadened, and we believe this is due to slow motion of this part of the lipid molecule. Although the spectra sharpen dramatically at the phase transition, the total breadth is roughly the same in both the L_β and L_α phases. We believe this indicates that the head group conformation is similar in both phases, even though the motional rates are substantially different.

Materials and Methods

Synthesis. [1-^{13}C]Palmitic acid was purchased from Kor Isotopes (Cambridge, MA). The synthesis of ^2H-labeled fatty acids is described elsewhere (Das Gupta et al., 1982). *sn*-2 chain labeled DPPE was prepared by reacylating *N*-(*tert*-butyloxycarbonyl)lysophosphatidylethanolamine with the respective fatty acid anhydride; *N*,*N*-dimethyl-4-aminopyridine was used as a catalyst (Chakrabarti & Khorana, 1975; Gupta et al., 1977). DPPE ^2H labeled in the C_2 position of the glycerol backbone was prepared by the following procedure: the pyridinium salt of *sn*-glycero-*2*-d_1-3-phosphate was reacylated with palmitic anhydride in the presence of *N*,*N*-dimethyl-4-aminopyridine as a catalyst (Gupta et al., 1977). The *N*,*N*-dimethyl-4-aminopyridinium salt of the resulting 1,2-dipalmitoyl-*sn*-glycero-*2*-d_1-3-phosphate was coupled with *N*-(*tert*-butyloxycarbonyl)ethanolamine by using triisopropylbenzenesulfonyl chloride as a condensing agent (Aneja et al., 1970; Kingsley & Feigenson, 1979). The removal of the N-protecting group, *N*-*tert*-butyloxycarbonyl, was achieved by treatment with anhydrous trifluoroacetic acid (Chakrabarti & Khorana, 1975). The synthesis of *sn*-glycero-*2*-d_1-3-phosphate will be described elsewhere (R.G. Wittebort et al., unpublished results). Head group labeled DPPE was prepared according to the procedure of Eibl (1978). 1,2-Dipalmitoyl-*sn*-glycerol was converted to 1,2-dipalmitoyl-*sn*-glycero-3-phosphoric acid dichloride by phosphorylation with phosphorus oxychloride and coupled to ethanolamine-*1*-d_2 by using triethylamine. Ethanolamine-*1*-d_2 was synthesized by reduction of glycine ethyl ester with $LiAlD_4$ (Weissbach & Sprinson, 1953).

NMR Spectroscopy. ^{13}C and ^2H spectra were obtained on a home-built solid-state pulse spectrometer operating at 6.8 T (73.9 MHz for ^{13}C, 45.1 MHz for ^2H, and 294 MHz for ^1H). ^{13}C spectra of DPPE in the liquid-crystalline phase were recorded with a Hahn spin-echo. For gel-state spectra cross-polarization with a 180° refocusing pulse at the ^{13}C frequency was used (Pines et al., 1973; Griffin, 1981) with a π pulse width of 6 μs. Sample heating due to ^1H decoupling was minimized by employing the minimum decoupling power necessary to obtain sharp spectra and long (5 s) recycle delays. From 500 to 5000 echos were accumulated for each ^{13}C spectrum.

^2H spectra were taken with the two-pulse quadrupole echo sequence (Solomon, 1958; Davis et al., 1976) using a pulse separation of 40 μs. The ^2H $\pi/2$ pulse width was 1.7–2.0 μs. Between 5000 and 30000 echos were accumulated with dwell times of 0.2–0.5 μs for gel-state spectra and 2 μs for liquid-crystalline-state spectra. Recycle delays were typically 0.25 s. Quadrature detection, as well as phase cycling, was used in all cases (Griffin, 1981).

Samples generally consisted of 50–100 mg of DPPE dispersed in an equal amount of deuterium-depleted water (Aldrich Chemicals, Milwaukee, WI) sealed in 7-mm glass tubes. Prior to the NMR experiments samples were equilibrated at 70 °C for 1 h. Because of the high equilibration

temperature, samples were checked by TLC before and after each NMR experiment for impurities or decomposition.

Temperature control was achieved with a gas flow system employing a platinum-resistance thermometer (Lake Shore Cryotronics, Westerville, OH), a Thor Cryogenics (Richmond, CA) controller, and a home-built power amplifier. The heated (or cooled) gas was blown directly onto the radio-frequency coil, which consisted of ~6 turns of heavy copper wire, which is an approximation to a constant-temperature oven. The temperature was controlled to ~1 °C, and we believe temperature gradients across the sample are of similar size.

^2H Absolute Intensity Spectra. Spectral simulations were performed with a program that will be discussed in detail elsewhere (R. G. Wittebort and R. G. Griffin, unpublished results), which includes corrections for power roll-off (Bloom et al., 1980) and spectral distortions resulting from use of the quadrupole echo (Spiess & Sillescu, 1981). As will be seen below, the echo-distortion calculations predict not only experimental line shapes but also the relative intensities of the ^2H spectra as a function of the jump rates. Where indicated, the ^2H spectra are plotted on an absolute intensity scale. Experimentally, absolute intensities were obtained by dividing the time domain signal by the number of scans and multiplying by a constant factor. This assumes that spectrometer sensitivity remains constant over the 0–70 °C temperature range studied, which in turn requires that probe Q change only slightly with temperature. Probe sensitivity was measured with a standard sample of solid valine-d_6, whose line shape and T_2 are nearly constant between 0 and 70 °C. Probe sensitivity decreased by approximately 15% at the higher temperature. Reproducible intensities at a given temperature may be obtained to within about 5% through careful attention to probe tuning. As will be seen, the absolute intensity changes due to molecular motion are large. For example, a factor of 2 decline at *lower* temperature for DPPE is easily distinguishable from the effects of probe response. Such changes contain information not necessarily available from the line shape, and a careful simulation of both line shapes and intensities can yield precise rates of motion when they are of interest. Although quadrupole echo intensity losses have been discussed theoretically (Spiess & Sillescu, 1981), the results presented here represent the initial confirmation of their existence.

Results and Discussion

^{13}C Spectra of 2[1-^{13}C]DPPE. In Figure 1 we show proton-decoupled ^{13}C spectra of 2[1-^{13}C]DPPE in 50 wt % H_2O as a function of temperature. The predominant signal in the spectrum at −55 °C is the slightly asymmetric rigid lattice powder pattern of the ^{13}C-enriched *sn*-2 carbonyl group. A spectrum of 2[1-^{13}C]DPPE in the form of a dry powder exhibits essentially the same features—e.g., a rigid lattice powder pattern with principle components $\sigma_{11} = -132$ ppm, $\sigma_{22} = -12$ ppm, and $\sigma_{33} = 11$ ppm, relative to external benzene. The signals on the right side of the spectra of Figure 1 arise from the natural abundance ^{13}C nuclei of the acyl chains, the head group, and the glycerol backbone, and are well separated from the $^{13}C{=}O$ powder pattern. At higher temperatures ($T \geq -15$ °C) the asymmetric powder pattern transforms into an axially symmetric pattern of reduced breadth. At 25 °C $\overline{\Delta\sigma} = 97$ ppm with the components $\sigma_{\parallel} = -112$ ppm and $\sigma_{\perp} = -15$ ppm, and the spectrum narrows slightly to 89 ppm at 60 °C. However, on passing through the gel to liquid-crystalline phase transition, the powder pattern collapses to a single line of ca. 150-Hz width (~2 ppm). Similar results have been observed for 2[1-^{13}C]DPPC, except that the transformation from the powder pattern to the narrow line occurs gradually, rather than precipitously, because of the existence of the P_{β} or $P_{\beta'}$ phase (Janiak et al., 1976, 1979; Stamatoff et al., 1982; Meier et al., 1982; Wittebort et al., 1981, 1982).

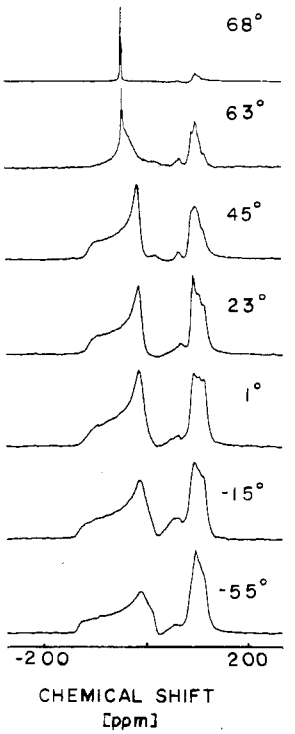

FIGURE 1: Proton-decoupled ^{13}C NMR spectra of 2[1-^{13}C]DPPE in 50 wt % water as a function of temperature. Shifts are relative to external benzene.

The temperature-dependent changes in the ^{13}C spectra can be explained with the following arguments, which are similar to those used previously for DPPC (Wittebort et al., 1981, 1982). At −55 °C the DPPE molecules show no appreciable motion on the ^{13}C NMR time scale, so that the rigid lattice powder pattern is observed. With increasing temperature, rotational diffusion of the whole molecule begins, and the asymmetric rigid lattice tensor is averaged to a fast-limit axially symmetric powder pattern of reduced breadth. For production of this spectrum, the motion must be faster than $\gamma H_0 \overline{\Delta\sigma} \simeq 10^4\ s^{-1}$. Furthermore, if we neglect the asymmetry in the rigid lattice tensor, then we can calculate the angle θ, between the unique tensor axis and the diffusion axis, according to

$$\overline{\Delta\sigma} = \Delta\sigma^{RL}\overline{(1/2)(3\cos^2\theta - 1)} \qquad (1)$$

where the bar denotes a temporal average and $\Delta\sigma^{RL}$ (=143 ppm) is the rigid lattice breadth. Using the values for $\overline{\Delta\sigma}$ above, we find $\theta \simeq 27°$ for DPPE at 25 °C. The collapse of the powder pattern to a single line above the phase transition can be explained by assuming that the molecule undergoes a conformational change at the phase transition, which fortuitously tilts the unique axis of the tensor to the magic angle (54.7°). The change in the spectral line shape observed at the phase transition cannot be due to an increase in the axial diffusion rates alone, since, as will be seen later, the ^2H chain labeled DPPE spectra indicate that the axial diffusion rates are already in the fast limit on the ^{13}C time scale. Furthermore, the ^2H spectra of the glycerol backbone labeled PE also indicate the existence of a conformational change in this region of the molecule at the phase transition.[2]

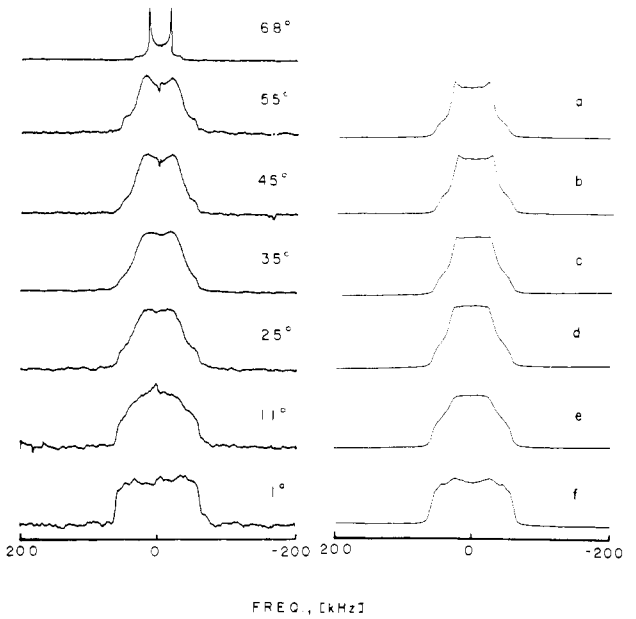

FIGURE 2: (Left) ^2H NMR spectra of 2[4,4-$^2H_2$]DPPE in 50 wt % water as a function of temperature. (Right) Line-shape simulations with R_R = rotational jump constant, R_{tg} = trans–gauche isomerization constant, and P_g = gauche probability: (a) $R_R = 7.5 \times 10^5$ s^{-1}, $R_{tg} = 8.5 \times 10^4$ s^{-1}, and $P_g = 0.07$; (b) $R_R = 6.25 \times 10^5$ s^{-1}, $R_{tg} = 7.3 \times 10^4$ s^{-1}, and $P_g = 0.06$; (c) $R_R = 5 \times 10^5$ s^{-1}, $R_{tg} = 5.4 \times 10^4$ s^{-1}, and $P_g = 0.06$; (d) $R_R = 4.5 \times 10^5$ s^{-1}, $R_{tg} = 4 \times 10^4$ s^{-1}, and $P_g = 0.05$; (e) $R_R = 3 \times 10^5$ s^{-1}, $R_{tg} = 3 \times 10^4$ s^{-1}, and $P_g = 0.04$; (f) $R_R = 2.1 \times 10^5$ s^{-1}, $R_{tg} = 2.7 \times 10^4$ s^{-1}, and $P_g = 0.02$.

The dynamical and conformational behavior of DPPE in the gel and liquid-crystalline phases appears to be similar to that observed for DPPC in that the *sn*-2 $^{13}C{=}O$ spectra in the L_β and $L_{\beta'}$ phases are nearly identical and in the L_α phase both lipids show a narrow ^{13}C line. However, as mentioned above, the two lipids do show differences in the details of the transformations between the two phases. Nevertheless, these results indicate that the conformations of PC and PE molecules in the region of the *sn*-2 C=O are probably quite similar in both the gel and liquid-crystalline phases. A similar conclusion was reached by Seelig & Browning (1978) for the liquid-crystalline phase by comparing residual quadrupole splittings of phospholipids ^2H labeled at the 2 position of the *sn*-2 chain.

Finally, we should mention that the ^{13}C spectrum at 63 °C, which is inside the phase-transition region, clearly shows a superposition of a sharp line and an underlying powder pattern. Similar spectra are observed at this temperature in the ^2H-labeled DPPE's (see Figures 2–4). Thus, signals arising from gel and liquid-crystalline domains can be observed separately, and the line shape indicates exchange between liquid and solid domains. The reason that the superposition line shapes are observed in the ^{13}C and ^2H spectra is the fact that the phase transitions in PE's are rather wide. For example, in chromatographically pure DPPE the half-width of the calorimetric endotherm is about 2 °C, and the onset of melting is observed at about 55 °C (Blume, 1980). Qualitatively similar spectra are observed in DPPC/DPPE mixtures (Blume et al., 1982)

[2] A reviewer has suggested that the collapse of the *sn*-2 $^{13}C{=}O$ spectrum could be due to diffusion around the surface of the liposomes. This is not a plausible explanation, since if it were correct, then, for example, the ^{31}P spectra of DPPE would also consist of isotropic-like lines. In fact, the ^{31}P spectra both above and below T_c consist of axially symmetric powder patterns of 40–60-ppm breadth (Seelig & Gally, 1976). A number of other possible explanations for the collapse of the *sn*-2 $^{13}C{=}O$ spectrum have been discussed elsewhere and also shown to be implausible (Wittebort et al., 1981, 1982).

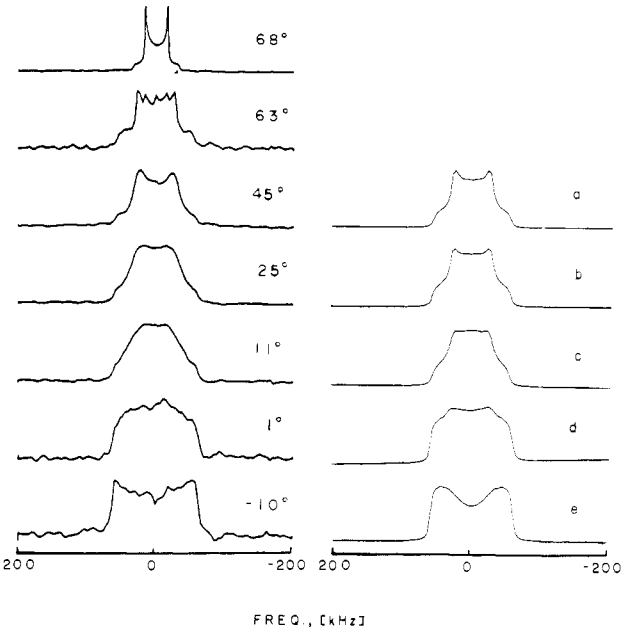

FIGURE 3: (Left) ^2H NMR spectra of 2[8,8-$^2H_2$]DPPE in 50 wt % water as a function of temperature. (Right) Line-shape simulations: (a) $R_R = 8.5 \times 10^5$ s^{-1}, $R_{tg} = 1.5 \times 10^5$ s^{-1}, and $P_g = 0.05$; (b) $R_R = 6 \times 10^5$ s^{-1}, $R_{tg} = 9 \times 10^4$ s^{-1}, and $P_g = 0.04$; (c) $R_R = 4.5 \times 10^5$ s^{-1}, $R_{tg} = 6 \times 10^4$ s^{-1}, and $P_g = 0.04$; (d) $R_R = 2.7 \times 10^5$ s^{-1}, $R_{tg} = 5 \times 10^4$ s^{-1}, and $P_g = 0.02$; (e) $R_R = 1.7 \times 10^5$ s^{-1}, $R_{tg} = 5 \times 10^4$ s^{-1}, and $P_g = 0.02$.

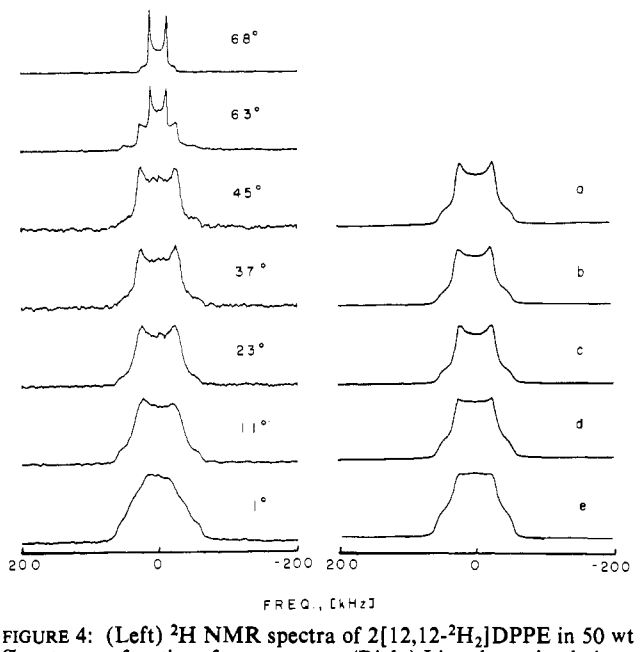

FIGURE 4: (Left) ^2H NMR spectra of 2[12,12-$^2H_2$]DPPE in 50 wt % water as a function of temperature. (Right) Line-shape simulations: (a) $R_R = 1.2 \times 10^6$ s^{-1}, $R_{tg} = 2 \times 10^5$ s^{-1}, and $P_g = 0.07$; (b) $R_R = 1 \times 10^6$ s^{-1}, $R_{tg} = 1.5 \times 10^5$ s^{-1}, and $P_g = 0.07$; (c) $R_R = 7.5 \times 10^5$ s^{-1}, $R_{tg} = 1 \times 10^5$ s^{-1}, and $P_g = 0.07$; (d) $R_R = 6.25 \times 10^5$ s^{-1}, $R_{tg} = 8.5 \times 10^4$ s^{-1}, and $P_g = 0.06$; (e) $R_R = 4.5 \times 10^5$ s^{-1}, $R_{tg} = 6 \times 10^4$ s^{-1}, and $P_g = 0.05$.

where again the calorimetric endotherms are wide (Blume, 1980). It is worth noting that commercially available PC's exhibit transition widths that are a factor of 4 smaller (0.5 °C) (Mabrey & Sturtevant, 1976). Moreover, with use of zone-refined fatty acids and with careful attention to other details of sample preparation, a further reduction of the endotherm width to 0.07 °C has been achieved (Albon & Sturtevant, 1978). It is possible that similar results could be obtained for PE's.

^2H Spectra of Acyl Chain Labeled DPPE. The top traces of Figures 2, 3, and 4 illustrate ^2H spectra of DPPE labeled at the 4, 8, and 12 positions, respectively, of the *sn*-2 chain in the liquid-crystalline phase. Qualitatively the spectra are very similar in that they are all fast-limit axially symmetric powder patterns, which indicate the presence of rapid axial diffusion of the whole molecule as well as fast gauche–trans isomerization. The residual quadrupole splittings at 68 °C are 31.5 kHz for the 4 position, 33.5 kHz for the 8 position, and 25.7 kHz for the 12 position. The splittings follow a pattern similar to that observed for phosphatidylcholines and phosphatidylserines in that the positions at the end of the chains have smaller splittings, indicating greater conformational freedom than in the middle part of the chain (Seelig & Seelig, 1974, 1975; Oldfield et al., 1978; Browning & Seelig, 1980). Nevertheless, there are some notable differences.

First, the residual quadrupole splittings in DPPE are generally larger than those observed in phosphatidylcholines, in DPPS, and in glycolipids (Huang et al., 1980). Second, the splittings observed for the 8 position are larger than for the 4 position, whereas in other phospholipids the differences are small; i.e., the 4 and 8 positions are in the plateau region of the order parameter profile. This suggests that the acyl chains in liquid-crystalline DPPE bilayers are subject to greater conformational constraints than in other phospholipids. This observation agrees well with results obtained from the respective monolayer systems, where it was found that PE monolayers are more condensed in the liquid-expanded phase than PC monolayers (Phillips & Chapman, 1968; Blume, 1979). It is possible that strong head group interactions via hydrogen bonds, as found in the crystal structure of DLPE (Hitchcock et al., 1974) and postulated for gel-state PE's (Nagle, 1976; Scott & Cheng, 1977), are retained to some extent in the liquid-crystalline phase and result in these larger splittings. These observations also agree with recent dilatometry data reported by Wilkinson & Nagle (1981). These authors found the specific volumes of PC and PE in the gel phase are almost identical and that the volume change at the transition is smaller for PE than for PC. This result clearly suggests a more condensed liquid-crystalline phase for PE than for PC.

It is generally assumed that in the gel state the acyl chains are in the all-trans conformation, and in the case of DPPE the gel phase has been classified L_β, since the chains are oriented perpendicular to the bilayer plane (McIntosh, 1980). If the DPPE molecules were executing axial diffusion about their long axis, then the breadth of the axially symmetric rigid lattice powder pattern would be reduced by a factor of about 2—e.g., $\Delta\nu_{Q\perp} \approx 62.5$ kHz—because the C–D vectors of the methylene groups are perpendicular to the long axis of the molecule. Moreover, if the diffusion rates were fast on the ^2H NMR time scale, then we would observe sharp axially symmetric patterns. Inspection of Figures 2–4 shows that the splittings are indeed reduced by a factor of about 2 from the rigid lattice values, but they do not display the sharp parallel and perpendicular edges characteristic of fast-limit spectra. Further decreases in temperature lead to broadening of the line shapes until at 1 °C almost flat-topped spectra are observed. Note, however, that the line shapes for spectra just below the T_c approach fast-limit axially symmetric spectra; this is especially evident in the case of 2[12,12-$^2H_2$]DPPE (Figure 4).

We have analyzed these spectral line shapes by computer simulations on the basis of the following model. The molecules are allowed to execute 3-fold (120°) rotational jumps around their long axis. This seems to be a more appropriate model for rotational diffusion in the gel state than a continuous-diffusion model. In particular, the chains are crystallized in a hexagonal lattice, and rotational, as well as lateral, diffusion probably proceeds via jumps from one lattice site to an adjacent unoccupied site, i.e., to a defect in the lattice. Because the molecules have two chains, these jumps may involve 60° rotations of the molecule. However, for symmetry reasons a three-site rotational jump model produces spectra identical with that of a six-site model and is sufficient. In addition to rotational jumps, trans–gauche isomerization is allowed; e.g., a particular C–D vector can jump between an orientation perpendicular to the long axis (90°) to a gauche site with an angle of 35.3° with respect to the long axis. Effectively, this leads to a six-site jump model with equal probabilities for the three sites of the rotational jump and variable probabilities for the trans and gauche sites. Different rate constants for rotational jumps and trans–gauche isomerization are possible, and corrections for power roll-off (Bloom et al., 1980) and echo distortions (Spiess & Sillescu, 1981) are included in the program. Corrections for probe response were smaller than experimental error and not included. A detailed description of the calculation procedure will be published elsewhere (R. J. Wittebort and R. G. Griffin, unpublished results). While this model is certainly a simplification of the real situation, the agreement between the simulations shown in Figures 2–4 and the experimental spectra is satisfactory.

The parameters used in the simulations are included in the figure captions, and we note that the rotational jump rates range from ca. 2×10^5 to 1.5×10^6 s^{-1}. These are intermediate rates on the ^2H NMR time scale, but for ^{13}C they satisfy the fast-limit condition. The gauche probabilities for the particular C–D vectors are relatively low, 0.07 or less, and they decrease at lower temperatures. A rough estimate for the gauche probability, P_g, at a particular position may be obtained from $\Delta\nu_{Q\parallel}$, the splitting of the parallel edges of the powder pattern. In the case of 2[4,4-$^2H_2$]DPPE we find 115 kHz at 25 °C, while for 2[8,8-$^2H_2$]DPPE $\Delta\nu_{Q\parallel}$ is 116.5 kHz and for 2-[12,12-$^2H_2$]DPPE $\Delta\nu_{Q\parallel}$ is 104 kHz. Thus, there is a clear increase of the gauche probability toward the end of the chain. Although the differences between the 4 and 8 positions are not large, the 8 position nevertheless does show the lowest gauche probability, suggesting tighter packing in the middle part of the chain. Thus, the gauche probability P_g in the gel state shows a similar dependence on the chain position to that observed in the liquid-crystalline state. In addition, a small temperature-dependent behavior is found; i.e., for the 4 position P_g increases from 0.05 at 25 °C to 0.07 at 55 °C, and for the 8 position the relative change is similar, 0.04 at 25 °C and 0.06 at 55 °C, while for the 12 position P_g is essentially constant, 0.07 at 25 °C and 0.08 at 53 °C. The uncertainties in the rotational jump rates, the gauche–trans isomerization rates, and P_g obtained from simulations are estimated to be ±5%, ±10%, and ±5%, respectively.

Parallel to the change in P_g, we observe an increase in the rotational jump rate, and both effects probably reflect the thermal expansion of the acyl chain lattice. Harlos (1978) measured the position of the wide-angle X-ray reflection in DSPE bilayers as a function of temperature. The line characteristic for the acyl chain lattice spacing shifts from 4.11 Å at 20 °C to a 4.24-Å position at 60 °C, and on the assumption of a hexagonal arrangement of the acyl chains, an area change of 6.4% can be calculated for this 40 °C range. This expansion of the lattice observed in the X-ray experiments could obviously facilitate rotational diffusion of the molecules as well as increased trans–gauche isomerization, and we find

that the area change resulting from kinks agrees with the X-ray data as the following arguments will show.

The occurrence of isolated gauche conformations in the gel state is highly unlikely because they lead to a bend in the acyl chain. Gauche bonds will probably be formed in pairs, i.e., as g^+tg^- kinks or g^+tttg^- jogs, which will lead to slight lateral displacement of the chain end below the kink (or jog) and to a reduction of the effective chain length (Seelig, 1977). Thus, the lateral expansion is partly compensated for by a reduction in bilayer thickness, and the dilatometry data of Wilkinson & Nagle (1981) appear to indicate that this assumption is basically correct. In particular, these authors observed a linear increase in specific volume with temperature. Extrapolation of their data leads to a volume change of 3.7% over the 40 °C range. This is definitely a lower value than the area change calculated from the X-ray spacings and is therefore consistent with the formation of kinks or jogs.

On the assumption of a constant gauche probability of 0.05 for all segments of the chain, ca. 0.375 g^+tg^- kinks per chain are present at any given time. With a reduction in chain length per kink of 1.25 Å (Seelig, 1977) we obtain an overall decrease in bilayer thickness of 0.94 Å compared to that of a strictly all-trans conformation. This value is probably too small to be detectable by low-angle X-ray diffraction, and similarly, the change in bilayer thickness over the 40 °C range is also too small to be detectable. However, the increase in area due to kink formation is more readily accessible. A g^+tg^- kink displaces the chain laterally by ca. 1.5 Å (Seelig, 1977), corresponding to an increase of the projected chain area of ~35%. For the 40 °C change in temperature we find a change in gauche probability of ca. 0.03 (see captions of Figures 2 and 3), corresponding to an increase in the number of kinks per chain of 0.225. The calculated area change per molecule resulting from kinks is ~7.8%, and this area compares favorably with the X-ray data of Harlos for DSPE, which yields an area change of 6.4%.

For a stiff rodlike molecule executing 3-fold jumps, the jump rates should be independent of the label position. However, when we compare the rotational jump rates obtained from the simulations of Figures 2–4, we see that the rates are higher when the label is farther down the chain. This apparent contradiction can be reconciled if it is remembered that the chains are flexible and can undergo torsional motions, which most likely affect positions near the terminal $-CH_3$. That the chains in phospholipids are not stiff rods has been observed in crystals of DMPC. In this case it was found that the orientation of the chain planes changes toward the methyl end, so that the chain is twisted to a certain degree (Pearson & Pascher, 1979). Similar conclusions have been drawn from Fourier-transform infrared studies of specifically ^{2}H-labeled DPPC by Cameron et al. (1981a,b). These authors analyzed the $-CD_2-$ stretching vibrations and found that the chain packing is more rigid in the middle part of the chain, i.e., at the 7 and 8 positions, than at either end. They suggested torsional oscillations of the whole chain as an explanation. In the context of the model that we have employed for the spectral simulations, these torsional oscillations appear as increased rotational diffusion and trans–gauche isomerization rates. A more elaborate line-shape model might be employed to account for coupled torsional oscillations among the $-CH_2-$ segments; however, in the absence of spectra from additional labeled positions, an analysis based on this type of model does not appear warranted. Nevertheless, the increases in the rotational jump rate and the trans–gauche isomerization rate observed in going from the 8 to the 12 position may reflect the presence of this type of motional averaging.

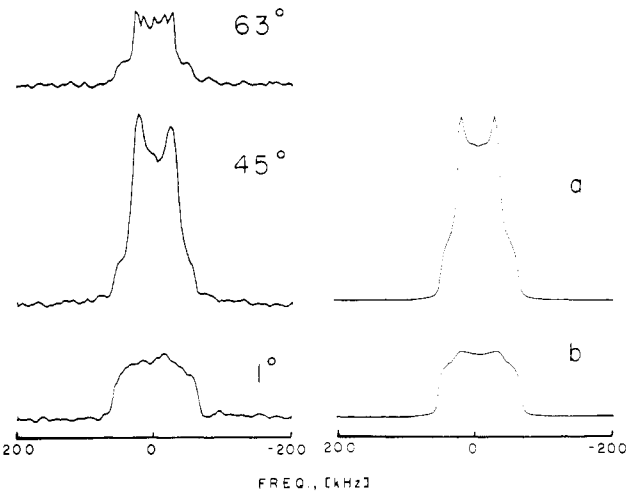

FIGURE 5: (Left) ^{2}H NMR spectra of 2[8,8-$^2H_2$]DPPE. (Right) Line-shape simulations plotted on an absolute intensity scale showing loss of spectral intensity when intermediate exchange rates are encountered. Simulation parameters are the same as those shown in legend of Figure 3 under (a) and (d).

Figure 5 illustrates another interesting feature observed in the ^{2}H chain labeled spectra. We mentioned above that the simulation program includes corrections for line-shape distortions induced by the quadrupole echo (Spiess & Sillescu, 1981; Rice et al., 1981a,b). These distortions are most pronounced when the motional correlation times are the same size as the reciprocal of the quadrupole interaction. In this situation the effective T_2 for certain portions of the powder pattern becomes very short, and magnetization from these regions is not refocused by the second $\pi/2$ pulse of the quadrupole-echo sequence. As a result the line shapes are distorted, and in the case of 3-fold axial jumps the effect is to remove intensity from the center of the spectrum. In addition, there is a decrease in the total intensity of the NMR signal, as is illustrated in Figure 5. Here we have plotted the experimental spectra for 2[8,8-$^2H_2$]DPPE, as well as the spectral simulations, on an absolute intensity scale. Note that the intensity of the 1 °C spectrum is reduced and that the loss is reproduced by the simulation with an intramolecular exchange rate $\sim 10^5$ s^{-1}. In contrast, at 45 °C the exchange rate is $\sim 10^6$ s^{-1}, which is approaching the fast limit, and the spectral intensity has increased.

In the phase-transition region at 63 °C we observed a second type of loss of intensity. In this case we believe it is due to intermolecular exchange. Inspection of Figures 3 and 5 suggests that the 2[8,8-$^2H_2$]DPPE line shape at 63 °C is a superposition of a liquid-crystalline and a gel-state spectrum, resulting from the presence of both types of lipid at $\sim T_c$. However, neither of these spectra alone should manifest the effects of echo distortions that are illustrated in Figure 5, since they are in both cases approximately fast-limit spectra. Therefore, the intensity loss in the phase-transition region must be due to a different mechanism, and we believe the most plausible explanation is exchange on an intermediate time scale between gel and liquid-crystalline domains. Because of the "echo distortion" effect, these exchanging molecules, which are probably limited to boundary regions between gel and liquid-crystalline phase domains, do not contribute their full intensity to the spectrum. The absence of their contribution is not obvious from the line shape itself and illustrates the importance of measuring absolute spectral intensities in such cases. The conclusions drawn from the quadrupole-echo in-

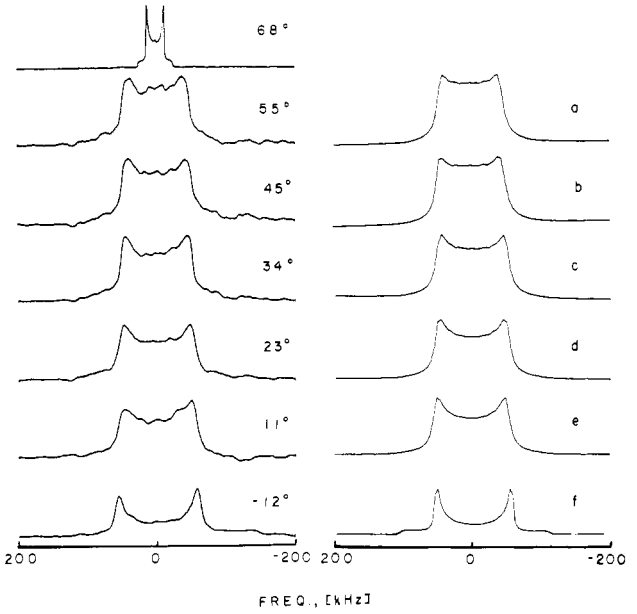

FIGURE 6: (Left) ^2H NMR spectra of [*glycerol*-C_2-^2H]DPPE in 50 wt % water as a function of temperature. (Right) Line-shape simulations with R_R = rotational jump rate constant, R_L = rate constant of torsional motion, and P_{15} = probability for 15° orientation (see text for explanation): (a) $R_R = 7.5 \times 10^5\ s^{-1}$, $R_L = 5.6 \times 10^4\ s^{-1}$, and $P_{15} = 0.4$; (b) $R_R = 6.25 \times 10^5\ s^{-1}$, $R_L = 4.8 \times 10^4\ s^{-1}$, and $P_{15} = 0.5$; (c) $R_R = 4.5 \times 10^5\ s^{-1}$, $R_L = 3.9 \times 10^4\ s^{-1}$, and $P_{15} = 0.6$; (d) $R_R = 3.8 \times 10^5\ s^{-1}$, $R_L = 3.7 \times 10^4\ s^{-1}$, and $P_{15} = 0.65$; (e) $R_R = 2.9 \times 10^5\ s^{-1}$, $R_L = 2.8 \times 10^4\ s^{-1}$, and $P_{15} = 0.7$; (f) $R_R = 1.45 \times 10^5\ s^{-1}$, $R_L = 1.8 \times 10^4\ s^{-1}$, and $P_{15} = 0.95$.

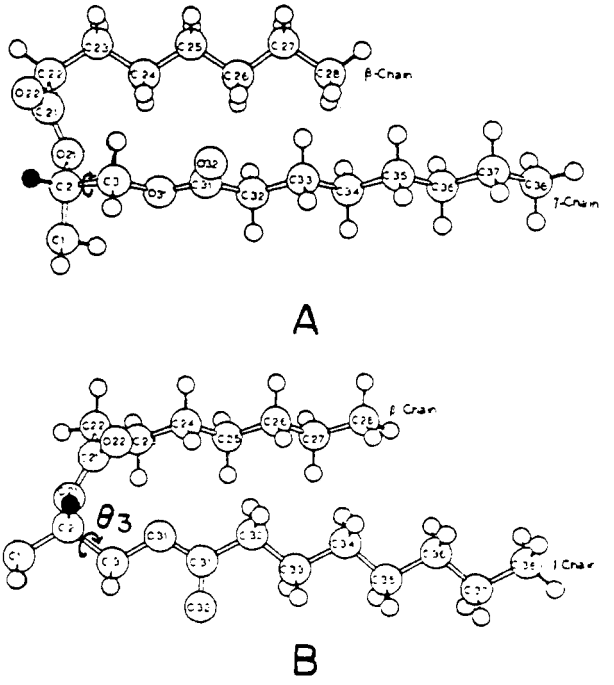

FIGURE 7: Molecular conformations of glycerol backbone and acyl chain regions according to McAlister et al. (1973). Conformation A seems to be preferred in gel-state lipids while conformation B was found in single crystals. Labeled glycerol backbone position is marked with a black dot. Notation of atoms and torsion angles is according to Sundaralingam (1972) and McAlister et al. (1973). For clarity the angle θ_3 is labeled only in part B of this figure.

tensities of Figure 5 are also in agreement with the *sn*-2 $^{13}C{=}O$ spectra of Figure 1 where it can be seen that the "solid" and "liquid" signals are clearly broadened by the exchange process. Similar effects have been observed in binary mixtures of PC and PE and PE and cholesterol (Blume et al., 1982; Blume & Griffin, 1982).

^2H Spectra of Glycerol Backbone Labeled DPPE. As we have seen above, ^2H spectra of chain-labeled DPPE's appear to be influenced by overall molecular diffusion, trans–gauche isomerization, and in the lower parts of the chain by torsional motions. In order to separate these effects more completely, we labeled DPPE at the C_2 position of the glycerol backbone, which we felt should be the most rigid part of the molecule. Figure 6 shows ^2H NMR spectra of this molecule together with some spectral simulations. Above the T_c the typical sharp, axially symmetric powder pattern characteristic of liquid-crystalline lipid is observed, while below the T_c the spectra are much wider and rounded due to intermediate exchange processes. The rotational jump rates used for the simulations of the gel-state spectra are nearly identical with those for 2-[4,4-$^2H_2$]DPPE. This is to be expected, since any additional torsional motion at the 4 position would be small and would therefore not lead to significant additional averaging. However, the splitting for the C_2 deuteron is remarkable in that it is large, roughly 95 kHz at 55 °C and 112 kHz at 11 °C. It is generally assumed that phospholipids in the gel phase adopt a conformation that is similar to that observed in single crystals of DLPE (Hitchcock et al., 1974) and DMPC (Pearson & Pascher, 1979), where the glycerol moiety is oriented perpendicular to the bilayer plane. In the crystalline state the glycerol backbone shows a trans conformation between the C_1–C_2 and C_2–C_3 bonds, which results in the C_2–D vector being oriented perpendicular to the long axis of the molecule. If this were the conformation in the gel phase, and diffusion were relatively fast, then we should observe spectra with $\Delta\nu_{Q\perp} \simeq 60$ kHz, as was the case for the chain. However, the splitting is much larger and we are forced to conclude that the average orientation of the C_2–D bond is not perpendicular to the long axis. If we neglect internal motion, then the angle between the director axis and the C_2–D vector must be ~24° at 55 °C and ~16° at 11 °C to account for the observed splittings.

Potential energy calculations by McAlister et al. (1973) show that two different conformations of the glycerol backbone have approximately the same energy minimum, and these are illustrated in Figure 7. In conformation A the angle θ_3 between the C_2 and C_3[3] carbons of the glycerol backbone is 60° while conformation B has $\theta_3 = 180°$. The B conformation is the one found in DLPE and DMPC single crystals, and the C_2–D bond is clearly perpendicular to the chain axis. In the A conformation the angle with the long axis is reduced to ~35°, if we assume an all-trans conformation of all following bonds along the γ chain. However, the torsion angle γ^1, between C_3 and the oxygen, is slightly less than 180°, which further decreases the angle between the C_2–D bond and the long axis of the molecule (McAlister et al., 1973). The spectral data in Figure 6 indicate that the preferred conformation for the phospholipids in the gel phase is probably similar to conformation A proposed by McAlister and is different from that observed in single crystals. At the moment it is not clear how the head group would be accommodated given this gauche conformation in the glycerol backbone. It should be mentioned that DMPC labeled at the C_2 position of the glycerol backbone gives the same type of spectrum below its pretransition temperature (R. J. Wittebort, unpublished results).

In the simulation of the experimental spectra it was necessary to include a slow 20° torsional motion of the C–D bond

[3] Notation is according to McAlister et al. (1973).

about its average value. In particular, a slow rate was required to reproduce the intensity of the zero-frequency portion of the spectrum, and torsional motion was used to explain the change in splitting with temperature. Simulation of torsional motion was accomplished by incorporating into the simulation a 2-fold jump between orientations with angles of 15° and 35° with respect to the diffusion axis. The increase in splitting with decreasing temperature was accounted for by changing the populations for the 15° and 35° sites as indicated in Figure 6. While this particular model may not be a unique solution, it does reproduce the observed spectral features quite well. In addition there are two other pieces of data that indicate that this type of model is physically plausible. First, ^2H spectra of DMPC labeled at the 1 position of the glycerol at −20 °C exhibit line shapes that can be interpreted in terms of a similar two-site hopping model (R. J. Wittebort, V. Rios-Mercadillo, R. G. Griffin, and G. M. Whitesides, unpublished results). In particular, the spectra show peaks at about ±60 and 0 kHz with a loss of intensity at frequencies between these singularities. This is the type of echo-distortion spectrum expected from slow two-site hopping on a tetrahedral lattice (Spiess & Sillescu, 1981). If this type of motion exists at the 1 position of the glycerol, then it is not unreasonable to expect some coupling to the 2 position. At the same time, the motion at the 2 position is expected to be constrained by the fact that the *sn*-2 chain is attached to this carbon. Second, high-resolution ^1H and ^{13}C spectra of short-chain lecithins, which form spherical micelles, show an equilibrium between gauche and trans conformations about the C_2–C_3 bond (Hauser et al., 1980). While the detailed conformation and rates of interconversion between conformations may be different in micelles and the liposomes studied here, the observation of the coexistence of these conformations supports the notion that there is some motion at the C_2 position in the gel state of DPPE.

Upon passage through the main transition the splitting decreases by about a factor of 4 to 26 kHz. The fact that the splitting changes so dramatically from that observed in the L_β phase indicates that there is a conformational change in the glycerol backbone at the phase transition. At the moment the details of this conformational change are not clear. However, the size of the splitting is not consistent with either the trans conformation observed in crystals or the gauche conformation, which we believe exists in the gel state. The fact that the L_α-phase ^2H spectra of all specifically ^2H-labeled lipids are axially symmetric powder patterns indicates that there is rapid axial diffusion about the director axis in this phase. Therefore, if the glycerol backbone were in the trans conformation observed in crystals (Figure 7B), then we would have observed a spectrum with $\Delta\nu_{Q\perp} \simeq 60$ kHz. Correspondingly, the gauche conformation (Figure 7A) would yield $\Delta\nu_{Q\perp} \simeq 90$ kHz. The observed 26-kHz splitting could be due to a single conformation different from that observed in either crystals or the gel phase. Alternatively, a rapid equilibrium among two or more weighted conformations could result in this spectrum. At the moment there is not sufficient spectral data available to differentiate among these possibilities.

A plot of the logarithm of the rotational jump rate constants obtained from the spectral simulations vs. $1/T$ shows a linear dependence. The activation energies determined from the slopes are approximately 4 kcal/mol. The rate constants obtained from simulations of spectra at higher temperatures are not very accurate because the fast-limit regime is approached; thus, data points for these temperatures depart from the linear plot. This is particularly the case for the simulations of 2[12,12-$^2H_2$]DPPE spectra above 25 °C. The lower jump rates observed for glycerol-labeled DPPE and 2[4,4-$^2H_2$]DPPE reflect the rotational motion of the whole molecule, which probably occurs via jumps into lattice defects.

If we apply a rotational random walk model to this motion, the rotational jump rate can be converted to a rotational diffusion rate, and we find for the mean square angular displacement $\langle\theta^2\rangle$:

$$\langle\theta^2\rangle = \Delta\theta^2 n = (2\pi/N)^2 n = (4\pi^2/N^2)kt \qquad (2)$$

where $\Delta\theta$ is the angular jump distance in radians, n is the number of jumps, N is the number of sites in the rotational jump model, and k is the jump rate constant. The relation between the Brownian rotational diffusion constant D_R and $\langle\theta^2\rangle$ is (Saffman & Delbrück, 1975)

$$\langle\theta^2\rangle = 2D_R t \qquad (3)$$

Combination of both equations gives

$$D_R = 2\pi^2 k/N^2 \qquad (4)$$

For a three-site rotational jump model $N = 3$, and we calculate at 25 °C that $D_R \simeq 8.8 \times 10^5$ s^{-1}. The rotational correlation time $\tau_c = 1/(6D_R)$, and we find a value for τ_c of 1.9×10^{-7} s. If the lipids were actually undergoing six-site jumps, the value of D_R would be a factor of 4 smaller or 2.2×10^5 s^{-1}. Saturation transfer electron spin resonance (STESR) has recently been employed to study long-axis rotation in lipid bilayer systems with a spin-labeled phospholipid (Marsh, 1980; Marsh & Watts, 1980). These authors report a value of 2×10^{-5} s for the effective rotational correlation time of this spin-label in DPPE bilayers at 15 °C. However, ^2H NMR data indicate rotational correlation times that are nearly 2 orders of magnitude shorter than those deduced from STESR. There appears to be no simple explanation for these differences. Rotational correlation times longer than 10^{-5} s would lead to rigid limit spectra in the case of ^2H NMR, with line shapes clearly different from those observed.

Lowering the temperature below 0 °C leads to a rapid decrease in the rate constants, and at −55 °C the rotational motion is essentially frozen out on both the ^2H and the ^{13}C NMR time scales (see Figure 1). However, if we assume an Arrhenius type behavior, we would extrapolate a rotational rate constant of $\sim 3.6 \times 10^4$ s^{-1} at −55 °C, which is still in the intermediate exchange regime on the ^{13}C NMR time scale. The discrepancy between this number and the experimental observations is probably due to the change in chain packing as found from X-ray diffraction experiments (Harlos, 1978) and recently verified by Fourier-transform IR studies (Cameron et al., 1981a,b).

The appearance of factor group splittings of the CH_2-scissoring bands is taken as an indication of a transition from a loose hexagonal to an orthorhombic packing of the acyl chains with a higher degree of interchain interactions. In DPPE these factor group splittings start to appear just above 0 °C and are fully developed at −60 °C. At the same temperature (0 °C) two wide-angle X-ray reflections appear, indicating a change in hydrocarbon chain packing. The conclusions drawn from these experiments agree with our observations, namely, that above 0 °C the chains have a relatively high degree of freedom for rotational and torsional motion, and that these motions are essentially frozen out by the transition from a hexagonal to a orthorhombic packing at lower temperatures.

^2H Spectra of Ethanolamine Head Group Labeled DPPE. In Figure 8 we present ^2H NMR spectra of DPPE labeled at

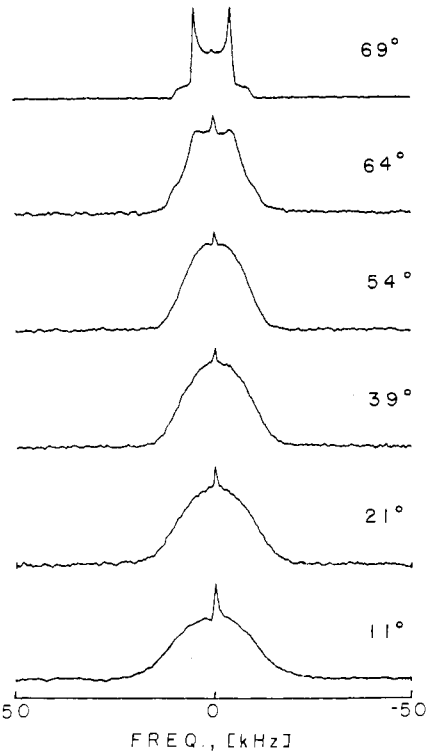

FIGURE 8: ^2H spectra of $^+NH_3$–CH_2–CD_2–DPPE in 50 wt % water as a function of temperature. Note that the width of the spectra is approximately the same in both the gel and liquid-crystalline phases.

the C_1 position of the ethanolamine head group. Above the T_c a sharp fast-limit powder pattern with a splitting of $\Delta\nu_{Q\perp}$ = 9.5 kHz is observed in agreement with earlier data of Seelig & Gally (1976). Below the transition a wide featureless line of ca. 16 kHz-total width appears. At lower temperatures the width of the spectrum increases to about 20 kHz, but the line shape does not change. Concurrently, there is a dramatic decrease in the intensity of the spectra with decreasing temperature, and at 0 °C the signal is essentially lost.

It is known from previous X-ray and neutron diffraction data that the phosphatidylethanolamine and choline head groups are oriented approximately parallel to the bilayer surface (Hitchcock et al., 1974; Griffin et al., 1978; Büldt & Seelig, 1980). Similar conclusions have been drawn from potential energy calculations (Sundaralingam, 1972; McAlister et al., 1973; Kovacs et al., 1980). However, the polar group can adopt several different conformations by rotations around the C_2–C_1 bond of the glycerol backbone as well as the two P–O diester bonds. For example, at least seven different stable conformers emerged from the calculations of Frischleder et al. (1981). As a result it is not possible to arrive at a unique solution for the motion of the head group, and, correspondingly, a unique spectral simulation (Skarjune & Oldfield, 1979). Nevertheless, the spectra do provide two pieces of semiquantitative information. First, the fact that the total width of the spectrum does not change substantially suggests that the number and angular extent of head group conformations in the gel phase are probably similar to those in the liquid-crystalline phase. Second, the loss of quadrupole-echo intensity indicates that the motion is pseudo-isotropic. The pseudo-isotropic character could arise exclusively from internal degrees of freedom, for example, gauche–trans isomerization, or from internal motions that occur perpendicular to the axial diffusion of the whole molecule. The loss of signal intensity with decreasing temperature suggests that some motions are in intermediate exchange, that is, of the order of the reciprocal of the rigid lattice quadrupole interactions or less. As has been pointed our previously (Spiess & Sillescu, 1981), isotropic motion is particularly effective in reducing echo intensities. The fact is best illustrated by the case of perdeuterated hexamethylenetetramine, which reorients by 4-fold tetrahedral jumps in the solid state. Because of this, it was not possible to obtain a quadrupole echo; instead, it was necessary to employ continuous wave NMR techniques in order to obtain the spectrum (Pschorn & Spiess, 1980). We believe that similar sorts of effects are present in the head group region of DPPE in the gel state.

Conclusions. Solid-state ^{13}C and ^2H NMR spectra can be used to characterize the structure and dynamic properties of phospholipids in both the gel and liquid-crystalline phases and the changes in these properties at this phase transition. However, as discussed above, investigations of the archetypical phospholipid diacyl-PC are complicated by the presence of the intermediate $P_{\beta'}$ phase, and therefore we have turned to the thermodynamically simpler system, DPPE. Since this phospholipid exists in a single L_β phase between 0 and 65 °C, it has permitted us to examine several spectral effects, and to unambiguously characterize its dynamic properties and its conformation in both the L_β and L_α phases.

The ^2H spectra of chain-labeled DPPE can be satisfactorily interpreted in terms of a model involving an approximately all-trans chain undergoing rotational diffusion (symmetry 3-fold or greater) at moderately fast rates (4×10^5 to 1.4×10^6 s^{-1}) on the ^2H NMR time scale. This model is derived from line-shape simulations and from the fact that the overall intensity of the spectrum changes with temperature. The latter result is a consequence of "echo distortions" and verifies that the observed spectra are due to rotational diffusion. It should be pointed out that the presence or absence of quadrupole echo distortions is an excellent, and necessary, test for a model based upon slow diffusion. The acyl chain ^2H spectra clearly do *not* show the 2 order of magnitude slower motion indicated by saturation transfer ESR experiments. Such slow motions would result in rigid lattice spectra with twice the width of those discussed here. Above the transition temperature the chain spectra are a factor of 2 narrower, and the line shapes are markedly sharper. This is best explained by an increase of gauche–trans isomerization as well as an increase in the rate of axial diffusion. For a CD_2 group fast-limit quadrupole echo spectra are obtained when the motional rates are greater than 10^7 s^{-1}; thus, the diffusion rates and the isomerization rates at least satisfy this criterion and may be faster.

The *sn*-2 $^{13}C{=}O$ spectra also support the rotational diffusion model, since in the L_β phase between 0 and 65 °C an axially symmetric fast-limit spectrum is observed. The more distinctive ^{13}C result is the complete collapse of the $^{13}C{=}O$ powder pattern at the gel to liquid-crystalline phase transition. The naive interpretation of this result, that the C=O carbon is undergoing isotropic motion, is clearly invalidated by the fact that all other labels and evidence show liquid-crystalline DPPE to exist in a bilayer. This leads to the conclusion that at the phase transition the glycerol region of the lipid undergoes a conformational change in which the unique axis of the shift tensor either is at, or is averaged about, the magic angle (54.7°) relative to the rotational diffusion axis. Similar changes are observed in the *sn*-2 $^{13}C{=}O$ spectra of lecithins, and thus this spectral change may be useful for detecting the presence of L_α phase phospholipids. It could obviously be used as a probe for the study of lipid mixtures and lipid–protein interactions.

The anomalously large quadrupole splitting of the deuteron at the glycerol 2 position indicates that this C–D bond is oriented between 15 and 35° relative to the rotational diffusion axis. This orientation can only be achieved when the C_2–C_3 glycerol bond is in a gauche conformation. Identical observations were made for DMPC below the pretransition, and together the observations indicate that the conformation in PE and PC crystals is not identical with that present in the gel state.

Spectra of head group labeled DPPE indicate that this part of the lipid molecule undergoes what may be characterized as pseudo-isotropic motion in both the L_β and L_α phases. We have not attempted to analyze this motion in detail because of the multiplicity of the conformations involved. Nevertheless, in both phases the residual coupling is an order of magnitude smaller than the rigid lattice ^2H breadth, and the gel-state spectra are dominated by pronounced line broadening and echo distortion intensity losses. These observations lead to the conclusion that the angular extent of the motions is qualitatively similar in both phases but that the rate in the L_β phase is slower by 3–4 orders of magnitude.

The results described here illustrate the utility of solid-state ^{13}C and ^2H NMR investigations of lipid bilayers. In particular, these techniques are nonperturbing and permit quantitative determinations of the mechanism and rate of dynamic processes, and the structural and conformational changes occurring at lipid phase transitions. Similar data are not easily obtained with other physical methods. The results reported here can serve as a basis for the analysis of other phospholipid systems—e.g., lipid–lipid or lipid–protein mixtures—where more complicated phase behavior and/or dynamic processes are to be expected.

References

Albon, N., & Sturtevant, J. M. (1978) *Proc. Natl. Acad. Sci. U.S.A. 75*, 2258.

Aneja, R., Chadha, J. S., & Davies, A. P. (1970) *Biochim. Biophys. Acta 218*, 102.

Bloom, M., Davis, J. H., & Valic, M. I. (1980) *Can. J. Phys. 58*, 1510.

Blume, A. (1979) *Biochim. Biophys. Acta 557*, 32.

Blume, A. (1980) *Biochemistry 19*, 4908.

Blume, A., & Ackermann, T. (1974) *FEBS Lett. 43*, 71.

Blume, A., & Griffin, R. G. (1982) *Biochemistry* (second paper of three in this issue).

Blume, A., Wittebort, R. J., Das Gupta, S. K., & Griffin, R. G. (1982) *Biochemistry* (third paper of three in this issue).

Browning, J. L., & Seelig, J. (1980) *Biochemistry 19*, 1262.

Büldt, G., & Seelig, J. (1980) *Biochemistry 19*, 6170.

Cameron, D. G., Casal, H. L., Mantsch, H. H., Boulanger, Y., & Smith, I. C. P. (1981a) *Biophys. J. 35*, 1.

Cameron, D. G., Gudgin, E. F., & Mantsch, H. H. (1981b) *Biochemistry 20*, 4496.

Chakrabarti, P., & Khorana, H. G. (1975) *Biochemistry 14*, 5021.

Chapman, D., Williams, R. M., & Ladbrooke, B. D. (1967) *Chem. Phys. Lipids 1*, 445.

Chapman, D., Urbina, J., & Keough, K. M. (1974) *J. Biol. Chem. 249*, 2512.

Chen, S. C., Sturtevant, J. M., & Gaffney, B. J. (1980) *Proc. Natl. Acad. Sci. U.S.A. 77*, 5060.

Das Gupta, S. K., Rice, D. M., & Griffin, R. G. (1982) *J. Lipid Res. 23*, 197.

Davis, J. H. (1979) *Biophys. J. 27*, 339.

Davis, J. H., Jeffrey, K. R., Bloom, M., Valic, M. I., & Higgs, T. P. (1976) *Chem. Phys. Lett. 42*, 390.

Eibl, H. (1978) *Proc. Natl. Acad. Sci. U.S.A. 75*, 4074.

Frischleder, H., Krahl, R., & Lehmann, E. (1981) *Chem. Phys. Lipids 28*, 291.

Griffin, R. G. (1981) *Methods Enzymol. 72*, 108.

Griffin, R. G., Powers, L., & Pershan, P. S. (1978) *Biochemistry 17*, 2718.

Gupta, C. M., Radakrishnan, R., & Khorana, H. G. (1977) *Proc. Natl. Acad. Sci. U.S.A. 74*, 4315.

Harlos, K. (1978) *Biochim. Biophys. Acta 511*, 348.

Hauser, H., Guyer, W., Pascher, I., Skrabal, P., & Sundell, S. (1980) *Biochemistry 19*, 366.

Hitchcock, P. B., Mason, R., Thomas, K. M., & Shipley, G. G. (1974) *Proc. Natl. Acad. Sci. U.S.A. 71*, 3036.

Huang, T-H., Skarjune, R. P., Wittebort, R. J., Griffin, R. G., & Oldfield, E. (1980) *J. Am. Chem. Soc. 102*, 7377.

Janiak, M. J., Small, D. M., & Shipley, G. G. (1976) *Biochemistry 15*, 4575.

Janiak, M. J., Small, D. M., & Shipley, G. G. (1979) *J. Biol. Chem. 254*, 6068.

Kingsley, P. B., & Feigenson, G. W. (1979) *Chem. Phys. Lipids 24*, 135.

Kovacs, A. L., Brosio, E., Conti, F., DiNola, A., & Napolitano, G. (1980) *Chem. Phys. Lipids 27*, 113.

Mabrey, S., & Sturtevant, J. M. (1976) *Proc. Natl. Acad. Sci. U.S.A. 73*, 3862.

Marsh, D. (1980) *Biochemistry 19*, 1632.

Marsh, D., & Watts, A. (1980) *Biochem. Biophys. Res. Commun. 94*, 130.

McAlister, J., Yathindra, N., & Sundaralingam, M. (1973) *Biochemistry 12*, 1189.

McIntosh, T. J. (1980) *Biophys. J. 29*, 237.

Meier, P., Blume, A., Ohmes, E., Neugebauer, F. A., & Kothe, G. (1982) *Biochemistry 21*, 526.

Nagle, J. F. (1976) *J. Membr. Biol. 27*, 233.

Oldfield, E., Meadows, M., Rice, D., & Jacobs, R. (1978) *Biochemistry 17*, 2727.

Overath, P., & Thilo, L. (1978) *Int. Rev. Biochem. 19*, 1.

Pearson, R. H., & Pascher, I. (1979) *Nature (London) 281*, 499.

Phillips, M. C., & Chapman, D. (1968) *Biochim. Biophys. Acta 163*, 301.

Pines, A., Gibby, M. G., & Waugh, J. S. (1973) *J. Chem. Phys. 59*, 569.

Pschorn, O., & Spiess, H. W. (1980) *J. Magn. Reson. 39*, 217.

Rice, D. M., Blume, A., Herzfeld, J., Wittebort, R. J., Huang, T-H., Das Gupta, S. K., & Griffin, R. G. (1981a) *Biomolecular Stereodynamics, Proceedings of a Symposium* (Sarma, R. H., Ed.) Vol. II, pp 255–270, Adenine Press, New York.

Rice, D. M., Wittebort, R. J., Griffin, R. G., Meirovitch, E., Stimson, E. R., Meinwald, Y. C., Freed, H. J., & Scheraga, H. A. (1981b) *J. Am. Chem. Soc. 103*, 7707.

Rothman, J. E., & Lenard, J. (1977) *Science (Washington, D.C.) 195*, 741.

Saffman, P. G., & Delbrück, M. (1975) *Proc. Natl. Acad. Sci. U.S.A. 72*, 3111.

Scott, H. L., Jr., & Cheng, W. H. (1977) *J. Colloid Interface Sci. 62*, 125.

Seelig, A., & Seelig, J. (1974) *Biochemistry 13*, 4839.

Seelig, A., & Seelig, J. (1975) *Biochim. Biophys. Acta 406*, 1.

Seelig, J. (1977) *Q. Rev. Biophys. 10*, 353.

Seelig, J., & Gally, H. (1976) *Biochemistry 15*, 5199.

Seelig, J., & Browning, J. L. (1978) *FEBS Lett. 92*, 41.

Seelig, J., & Seelig, A. (1980) *Q. Rev. Biophys. 13*, 19.

Skarjune, R., & Oldfield, E. (1979) *Biochemistry 18*, 5903.
Solomon, I. (1958) *Phys. Rev. 110*, 61.
Spiess, H. W., & Sillescu, H. (1981) *J. Magn. Reson. 42*, 381.
Stamatoff, J., Feuer, B., Guggenheim, H., Tellez, G., & Yamane, T. (1982) *Biophys. J. 38*, 217.
Sundaralingam, M. (1972) *Ann. N.Y. Acad. Sci. 195*, 324.
Vaughan, D. J., & Keough, K. M. (1974) *FEBS Lett. 47*, 158.
Weissbach, H., & Sprinson, D. B. (1953) *J. Biol. Chem. 203*, 1031.
Wilkinson, D. A., & Nagle, J. F. (1981) *Biochemistry 20*, 187.
Wittebort, R. G., Schmidt, C. F., & Griffin, R. G. (1981) *Biochemistry 20*, 4223.
Wittebort, R. G., Blume, A., Huang, T-H., Das Gupta, S. K., & Griffin, R. G. (1982) *Biochemistry 21*, 3487.

Carbon-13 and Deuterium Nuclear Magnetic Resonance Study of the Interaction of Cholesterol with Phosphatidylethanolamine†

A. Blume‡ and R. G. Griffin*

ABSTRACT: Mixtures of dipalmitoylphosphatidylethanolamine (DPPE) and cholesterol (CHOL) have been studied with solid-state ^{13}C and ^{2}H nuclear magnetic resonance (NMR) techniques. DPPE was ^{13}C labeled at the carbonyl group of the *sn*-2 chain, and ^{2}H was introduced at the 4 position of the *sn*-2 chain and the 1 position of the ethanolamine head group. The ^{13}C and ^{2}H spectra of each labeled lipid were studied as a function of temperature and CHOL concentration, and the results indicate three distinguishable temperature–composition regions. In region I, which occurs at low temperatures and CHOL concentrations, the ^{13}C and ^{2}H spectra are similar to those observed for pure DPPE in its gel phase. In region II, which occurs at higher temperatures or CHOL concentrations, the *sn*-2 $^{13}C{=}O$ spectra of DPPE/CHOL mixtures display two components, indicating the coexistence of two conformationally and dynamically inequivalent DPPE molecules. One of these is similar to gel-state DPPE, while the second "fluid" fraction displays some liquid-crystalline character. The two-component ^{13}C spectra can be simulated quantitatively with a two-parameter chemical exchange model that permits the fraction of each form and the exchange rate to be determined as a function of temperature and composition. The ^{2}H spectra observed in region II do not exhibit two components in an obvious way. Nevertheless, with some reasonable assumptions, the ^{2}H spectra obtained from chain-labeled DPPE can also be simulated with a two-component model with the exchange rates and fractional populations obtained from the ^{13}C results. The calculations predict not only the line shapes but also the losses in spectral intensity arising from use of the quadrupole echo technique. Furthermore, the ^{2}H spectra show that with increasing temperature the fluid fraction observed in region II undergoes a transition to a higher degree of disorder, and should therefore not be labeled "liquid crystalline". In region III, which occurs at high temperatures and CHOL concentrations, both the ^{13}C and ^{2}H spectra are those expected of liquid-crystalline lipid. The NMR results are compared to, and found to be different from, those obtained with calorimetric investigations. It is suggested that these differences are due to the small domains present in DPPE/CHOL mixtures that lead to phase transitions of low cooperativity. Some metastability of the DPPE/CHOL system was observed at high CHOL concentrations and low temperatures.

Cholesterol (CHOL)[1] occurs in many biological membranes at relatively high levels, and as a consequence the properties of phospholipid/CHOL mixtures have been extensively investigated [for a review, see Demel & deKruijff (1976)]. Generally, the addition of CHOL to PC bilayers leads to a broadening of the gel to liquid-crystalline phase transition and to a decrease of the calorimetrically observed transition enthalpy (Ladbrooke et al., 1968). Recently, high-sensitivity DSC experiments have indicated that this transition is observable at CHOL concentrations up to about 50 mol % (Mabrey et al., 1978; Estep et al., 1978). Moreover, monolayer experiments have shown that addition of CHOL to liquid crystalline phase lipids can result in a condensation of the lipid lattice (Shah & Schulman, 1967; Phillips, 1972, Müller-Landau & Cadenhead, 1979). Thus, a simple and commonly used interpretation of the DSC and monolayer experiments is that CHOL orders the liquid-crystalline phase and disorders the gel phase of phospholipid bilayers. Nevertheless, a number of other more subtle effects have been observed in lipid/CHOL mixtures, and as a result there have been numerous investigations devoted to understanding the detailed features of PC/CHOL phase diagrams (Shimshick & McConnell, 1973; Estep et al., 1978; Mabrey et al., 1978; Gershfeld 1978; Pink & Chapman, 1979; Rubinstein et al., 1979, 1980; Lentz et al., 1980; Copeland & McConnell, 1980; Cornell et al., 1979; Owicki & McConnell, 1980; Melchior et al., 1980; Snyder & Friere, 1980; Recktenwald & McConnell, 1981).

Because most studies have focused on PC/CHOL mixtures, there is a paucity of information available on other phospholipid/CHOL systems. For example, it is only in the recent

† From the Francis Bitter National Magnet Laboratory, Massachusetts Institute of Technology, Cambridge, Massachusetts 02139. *Received April 20, 1982.* This research was supported by the National Institutes of Health (GM 23289, GM 25505, and RR00995) and by the National Science Foundation through its support of the Francis Bitter National Magnet Laboratory (C-670). A.B. was supported by a research scholarship from the Deutsche Forschungsgemeinschaft (BL 182/2 4).

‡ Present address: Institut für physikalische Chemie II, D-7800 Freiburg, Federal Republic of Germany.

[1] Abbreviations: CHOL, cholesterol; DPPC, dipalmitoylphosphatidylcholine; DPPE, dipalmitoylphosphatidylethanolamine; NMR, nuclear magnetic resonance; ESR, electron spin resonance; DSC, differential scanning calorimetry; TLC, thin-layer chromatography.

0006-2960/82/0421-6230$01.25/0